

A lowest order divergence-free finite element on rectangular grids

Yunqing Huang* and Shangyou Zhang

Abstract

It is shown that the conforming $Q_{2,1;1,2}$ - Q'_1 mixed element is stable, and provides optimal order of approximation for the Stokes equations on rectangular grids. Here $Q_{2,1;1,2} = Q_{2,1} \times Q_{1,2}$ and $Q_{2,1}$ denotes the space of continuous piecewise-polynomials of degree 2 or less in the x direction but of degree 1 in the y direction. Q'_1 is the space of discontinuous bilinear polynomials, with spurious modes filtered. To be precise, Q'_1 is the divergence of the discrete velocity space $Q_{2,1;1,2}$. Therefore, the resulting finite element solution for the velocity is divergence-free pointwise, when solving the Stokes equations. This element is the lowest order one in a family of divergence-free element, similar to the families of the Bernardi-Raugel element and the Raviart-Thomas element.

Keywords. mixed finite element, Stokes, divergence-free element, quadrilateral element, rectangular grids.

AMS subject classifications (2000). 65M60, 65N30, 76D07.

1 Introduction

In the finite element methods for computing incompressible flows, such as Stokes or Navier-Stokes flows, the incompressibility condition is usually enforced weakly, cf. [21, 8]. In order to satisfy the inf-sup stability condition, the incompressibility condition is weakened often by enlarging the finite element space for the velocity or decreasing the space for the pressure. This does not only waste computational work, but also lead to inaccurate mass conservation, especially in a long time range computation, and to large local errors. A natural approach would be choosing the divergence of the finite element space for the velocity as the space for the pressure. This would generate a divergence-free finite element, i.e., the incompressibility condition holds exactly for the finite element solution. Nevertheless, the method does not work when commonly used finite elements are used for the velocity, known as a type of locking.

A fundamental study on the method was done by Scott and Vogelius ([23, 24]) that the P_{k+1} - P_k^{dc} method is stable and consequently of the optimal order on 2D triangular grids, for $k \geq 3$. Here the velocity space is the continuous piecewise-polynomials of degree $(k+1)$ or less while the the pressure space is the discontinuous piecewise-polynomials of degree k or less, or the divergence of the velocity, to be precise. There are several other such divergence-free finite elements, cf. [2, 18, 20, 29, 30, 31].

In this manuscript, we propose a new, low-order, divergence-free element on rectangular grids, extending the family of divergence-free elements in [31]. This is the lowest order element in the family, and of most interest. The velocity space is the continuous $Q_{2,1} \times Q_{1,2}$ space,

*The work of the first author is supported in part by the NSFC for Distinguished Young Scholars(10625106) and National Basic Research Program of China under the grant 2005CB321701.

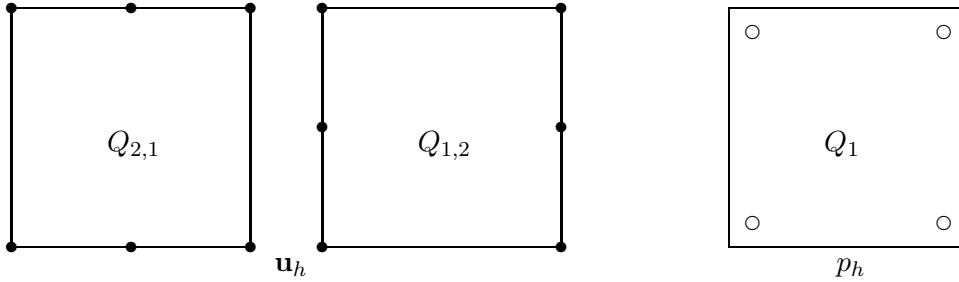


Figure 1: Degrees of freedoms for the velocity \mathbf{u}_h and the pressure p_h .

i.e., the first component of velocity is a piecewise polynomial of degree 2 in x direction but degree 1 in y direction while the second component is a rotation of the first one. The pressure space is the subspace of discontinuous bilinear polynomials, the divergence of the velocity, to be explicitly. The nodal degrees of freedom of the finite element pair are shown in Figure 1. We note that it is not new to use different polynomial degrees in different directions, when solving partial differential equations involving $\nabla \cdot$ and curl operators, cf. [27, 16]. The stability and the optimal order convergence will be proved for the new divergence-free element.

There is a long series of work on Q_k mixed finite elements on rectangular grids in 2D and 3D. In [27], Stenberg and Suri showed the stability, but a sub-optimal order of approximation, for the Q_{k+1} - Q_{k-1}^{dc} element for all $k \geq 1$ in 2D. Bernardi and Maday proved the stability and the optimal order of convergence for the Q_{k+1} - P_k^{dc} element, cf. [4]. Ainsworth and Coggins established [1] the stability and the optimal order of convergence for the Taylor-Hood Q_{k+1} - Q_k element, where the pressure space is continuous too. Brezzi and Falk showed that the Q_{k+1} - Q_k^{dc} element is unstable in [9], for any $k \geq 0$. The new divergence-free method is an optimization of the unstable Q_2 - Q_1^{dc} element, shown unstable by Brezzi and Falk. Here we decrease the Q_2 space for the velocity to $Q_{2,1,1,2}$. This reduces the dimension of velocity by a factor of 2. Meanwhile, we decrease the space Q_1^{dc} for the pressure to Q'_1 , by removing all spurious modes, i.e., eliminating one degree of freedom at each vertex. We have to emphasize that the discrete pressure space is introduced for the analysis, but not in the computation. By an iterated penalty method, we obtain the discrete solutions for the pressure without coding the pressure element, as the pressure solution is a byproduct, cf. [30] and Section 4 below. This is an advantage of the divergence-free element, which is not carried to other mixed-finite elements, neither to nonconforming (discontinuous) locally-divergence-free elements [6, 10, 12, 15, 14, 17, 28].

The new $Q_{2,1,1,2}$ element is similar to two other finite elements, the Bernardi-Raugel element and the Raviart-Thomas element. The Bernardi-Raugel element has the same structure for the velocity approximation, i.e., the $Q_{2,1,1,2}$ velocity space, but the Q_0 pressure space, cf. [5, 27]. So the element is not divergence free and loses one order of approximation in theory. The Raviart-Thomas element also has the same structure for the velocity space, $Q_{2,1,1,2}$. But the space is of discontinuous, or an $H(\nabla \cdot)$ space, to be exact, cf. [22].

The rest of the paper is organized as follows. In Section 2, we define the finite element for the Stationary Stokes equations. In Section 3, we show the inf-sup condition and the optimal order convergence for the newly proposed $Q_{2,1,1,2}$ element. In Section 4, we provide some test results confirming the analysis. We also make a numerical comparison with the most popular Q_1/P_0 element.

2 The $Q_{2,1;1,2}$ divergence-free element

In this section, we shall define the new finite element for the stationary Stokes equations on rectangular grids. The resulting finite element solutions for the velocity are divergence-free point wise.

We consider the stationary Stokes flow: Find the velocity \mathbf{u} and the pressure p on a 2D polygonal domain Ω , which can be subdivided into rectangles, such that

$$\begin{aligned} -\Delta \mathbf{u} + \nabla p &= \mathbf{f} && \text{in } \Omega, \\ \nabla \cdot \mathbf{u} &= 0 && \text{in } \Omega, \\ \mathbf{u} &= \mathbf{0} && \text{on } \partial\Omega. \end{aligned} \quad (2.1)$$

The weak form for (2.1) is: Find $\mathbf{u} \in H_0^1(\Omega)^2$ and $p \in L_0^2(\Omega) := L^2(\Omega)/C = \{p \in L^2 \mid \int_{\Omega} p = 0\}$ such that

$$\begin{aligned} a(\mathbf{u}, \mathbf{v}) + b(\mathbf{v}, p) &= (\mathbf{f}, \mathbf{v}) \quad \forall \mathbf{v} \in H_0^1(\Omega)^2, \\ b(\mathbf{u}, q) &= 0 \quad \forall q \in L_0^2(\Omega). \end{aligned} \quad (2.2)$$

Here $H_0^1(\Omega)^2$ is the subspace of the Sobolev space $H^1(\Omega)^2$ (cf. [11]) with zero boundary trace, and

$$\begin{aligned} a(\mathbf{u}, \mathbf{v}) &= \int_{\Omega} \nabla \mathbf{u} \cdot \nabla \mathbf{v} \, dx, \\ b(\mathbf{v}, p) &= - \int_{\Omega} \nabla \cdot \mathbf{v} \, p \, dx, \\ (\mathbf{f}, \mathbf{v}) &= \int_{\Omega} \mathbf{f} \cdot \mathbf{v} \, dx. \end{aligned}$$

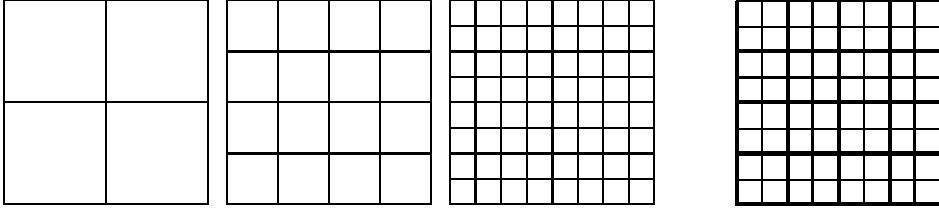


Figure 2: Three levels of nestedly refined grids, and a macro-element grid.

The finite element grids are defined by, cf. Figure 2,

$$\mathcal{T}_h = \{K \mid \cup K = \overline{\Omega}, K = [x_a, x_b] \times [y_c, y_d] \text{ with size } h_K = \max\{x_b - x_a, y_d - y_c\} \leq h\}.$$

We further assume, though the analysis can be easily extended to the general case, that the rectangles in grid \mathcal{T}_h can be combined into groups of four to form a macro-element grid:

$$\mathcal{M}_h = \{M \mid M = \cup_{i=1}^4 K_i = [x_{i-1}, x_{i+1}] \times [y_{j-1}, y_{j+1}], K_i \in \mathcal{T}_h, \cup K_i = \Omega\}.$$

See the 4th diagram in Figure 2. Let the polynomial spaces $Q_{2,1}$, $Q_{1,2}$ and Q_1 be defined by

$$Q_{k,l} = \left\{ \sum_{i \leq k, j \leq l} c_{ij} x^i y^j \right\}, \quad Q_k = Q_{k,k}.$$

The $Q_{2,1;1,2}$ mixed element spaces are

$$\mathbf{V}_h = \{ \mathbf{v}_h \in C(\Omega)^2 \mid \mathbf{v}_h|_K \in Q_{2,1} \times Q_{1,2} \ \forall K \in \mathcal{T}_h, \text{ and } \mathbf{u}_h|_{\partial\Omega} = 0 \}, \quad (2.3)$$

$$P_h = \{ \nabla \cdot \mathbf{u}_h \mid \mathbf{u}_h \in \mathbf{V}_h \}. \quad (2.4)$$

Since $\int_{\Omega} p_h = \int_{\Omega} \nabla \cdot \mathbf{u}_h = \int_{\partial\Omega} \mathbf{u}_h = 0$ for any $p_h \in P_h$, we conclude that

$$\mathbf{V}_h \subset H_0^1(\Omega)^2, \quad P_h \subset L_0^2(\Omega),$$

i.e., the mixed-finite element pair is conforming. The resulting system of finite element equations for (2.2) is: Find $\mathbf{u}_h \in \mathbf{V}_h$ and $p_h \in P_h$ such that

$$\begin{aligned} a(\mathbf{u}_h, \mathbf{v}) + b(\mathbf{v}, p_h) &= (\mathbf{f}, \mathbf{v}) \quad \forall \mathbf{v} \in \mathbf{V}_h, \\ b(\mathbf{u}_h, q) &= 0 \quad \forall q \in P_h. \end{aligned} \quad (2.5)$$

Traditional mixed-finite elements require the inf-sup condition to guarantee the existence of discrete solutions. As (2.4) provides a compatibility between the discrete velocity and discrete pressure spaces, the linear system of equations (2.5) always has a unique solution, cf. [30]. Furthermore, such a solution \mathbf{u}_h is divergence-free: by the second equation in (2.5) and the definition of P_h in (2.4),

$$b(\mathbf{u}_h, q) = b(\mathbf{u}_h, -\nabla \cdot \mathbf{u}_h) = \|\nabla \cdot \mathbf{u}_h\|_{L^2(\Omega)}^2 = 0. \quad (2.6)$$

In this case, we call the mixed finite element a divergence-free element. It is apparent that the discrete velocity solution is divergence-free if and only if the discrete pressure finite element space is the divergence of the discrete velocity finite element space, i.e., (2.4).

We note that by (2.4), P_h is a subspace of discontinuous, piecewise bilinear polynomials. As singular vertices are present (see [23, 24]), P_h is a proper subset of the discontinuous piecewise Q_1 polynomials. It is possible, but difficult to find a local basis for P_h . But on the other side, it is the special interest of the divergence-free finite element method that the space P_h can be omitted in computation and the discrete solutions approximating the pressure function in the Stokes equations can be obtained as byproducts, if an iterated penalty method is adopted to solve the system (2.5), cf. [13, 8, 7, 26, 30] for more information.

3 The stability

The central task is to prove the inf-sup condition, or the LBB condition ([21, 8]), for the discrete finite element spaces:

$$\inf_{0 \neq q \in P_h} \sup_{\mathbf{v} \in \mathbf{V}_h} \frac{b(\mathbf{v}, q)}{\|\mathbf{v}\|_{H^1} \|q\|_{L^2}} \geq C, \quad (3.1)$$

for some constant $C > 0$ independent of the grid size h . We will construct a velocity \mathbf{v} in four steps for a given discrete pressure $q \in P_h$. \mathbf{v}_1 will match the integrals $\int_M q$ on each macro-element, constructed globally. \mathbf{v}_2 will be constructed locally so that $\nabla \cdot \mathbf{v}_2$ match $q - \nabla \cdot \mathbf{v}_1$ at all four vertices of macro-elements. \mathbf{v}_3 will be constructed to match $q - \nabla \cdot (\mathbf{v}_1 + \mathbf{v}_2)$ at all mid-edge points of macro-elements. \mathbf{v}_4 will be constructed within each macro-element to match $q - \nabla \cdot (\mathbf{v}_1 + \mathbf{v}_2 + \mathbf{v}_3)$ at the center point of the macro-element.

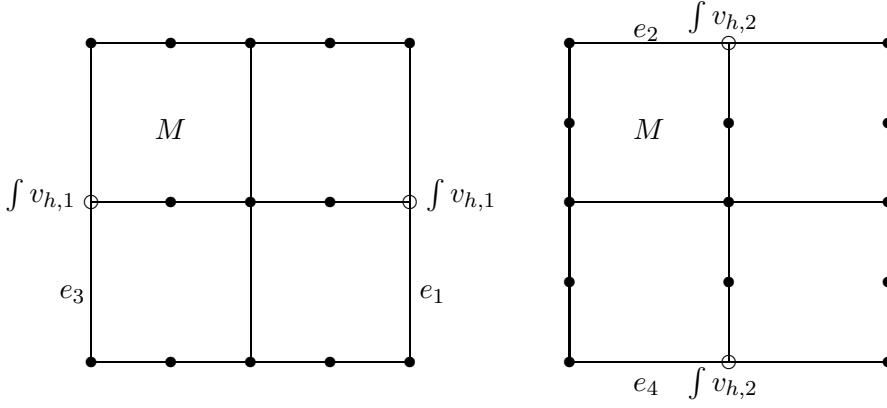


Figure 3: The two components $v_{h,1}$ and $v_{h,2}$ of \mathbf{v}_h on a macro-element M .

Lemma 3.1 For any $q \in P_h$ defined in (2.4), there is a function $\mathbf{v}_1 \in \mathbf{V}_h$ such that

$$\int_M \nabla \cdot \mathbf{v}_1 = \int_M q \quad \forall M \in \mathcal{M}_h, \quad \text{and} \quad \|\mathbf{v}_1\|_{H^1(\Omega)^2} \leq C\|q\|_{L^2(\Omega)}. \quad (3.2)$$

Proof. For any $q \in P_h$, by the theory on regular inversion of the divergence operator developed by Arnold, Scott and Vogelius in [3], there is a $\mathbf{u}_q \in H^{1+\alpha}(\Omega)^2 \cap H_0^1(\Omega)^2$ such that

$$\nabla \cdot \mathbf{u}_q(x, y) = q(x, y) \quad \text{a. e. for } (x, y) \in \Omega,$$

and

$$\|\mathbf{u}_q\|_{H^1} \leq C\|q\|_{L^2},$$

for any $0 < \alpha < 1/2$. Let the nodal interpolant be $\mathbf{v}_1 = \mathbf{I}_h \mathbf{u}_q$ where the interpolation operator \mathbf{I}_h is defined by nodal values except the integral values at mid-edge points of macro-element (cf. Figure 3):

$$\begin{aligned} \int_{e_i} u_{q,1} ds &= \int_{e_i} v_{h,1} ds, & i = 1, 3, \\ \int_{e_i} u_{q,2} ds &= \int_{e_i} v_{h,2} ds, & i = 2, 4, \end{aligned}$$

where

$$\mathbf{u}_q = (u_{q,1} \quad u_{q,2})^T, \quad \mathbf{v}_1 = (v_{h,1}, v_{h,2})^T.$$

Such a nodal interpolation is stable, cf. [25] for example, that

$$\|\mathbf{I}_h \mathbf{u}_q\|_{H^1(\Omega)^2} \leq C\|\mathbf{u}_q\|_{H^1(\Omega)^2}.$$

Further, the interpolant also preserve the divergence on each macro-element:

$$\begin{aligned} \int_M \nabla \cdot \mathbf{v}_1 dx dy &= \int_{\partial M} \mathbf{v}_1 \cdot \mathbf{n} ds \\ &= \int_{e_1} v_{h,1} ds + \int_{e_2} v_{h,2} ds - \int_{e_3} v_{h,1} ds - \int_{e_4} v_{h,2} ds \\ &= \int_{e_1} u_{q,1} ds + \int_{e_2} u_{q,2} ds - \int_{e_3} u_{q,1} ds - \int_{e_4} u_{q,2} ds \\ &= \int_M \nabla \cdot \mathbf{u}_q dx dy = \int_M q dx dy, \end{aligned}$$

cf. Figure 3. ■

After matching the integral value of q on each macro-element M by $\nabla \cdot \mathbf{v}_1$, we next match the four vertex-values of $q - \nabla \cdot \mathbf{v}_1$ on M .

Lemma 3.2 *For any $q \in P_h$ defined in (2.4) such that $\int_M q = 0 \quad \forall M \in \mathcal{M}_h$, there is a function $\mathbf{v}_2 \in \mathbf{V}_h$ such that*

$$\nabla \cdot \mathbf{v}_2(a_i^M) = q(a_i^M) \quad \forall M \in \mathcal{M}_h, \quad (3.3)$$

$$\int_M \nabla \cdot \mathbf{v}_2 = 0 \quad \forall M \in \mathcal{M}_h, \quad (3.4)$$

$$\|\mathbf{v}_2\|_{H^1(\Omega)^2} \leq C\|q\|_{L^2(\Omega)}. \quad (3.5)$$

Here a_i^M , $1 \leq i \leq 4$, are the four vertices of macro-element M .

Proof. According to Scott and Vogelius [23], all vertices in \mathcal{T}_h are singular, which means a function $q \in P_h$, because $q = \nabla \cdot \mathbf{w}_h$ for some $\mathbf{w}_h \in \mathbf{V}_h$, is subject to a minor continuity constraint:

$$\sum_{i=1}^4 (-1)^i q(a_i^{K_i}) = 0, \quad (3.6)$$

where $a_i^{K_i}$ are the vertices of four elements K_i meeting at an internal vertex, shown in Figure 4. But, at a boundary vertex A or B , when less than four squares meet, see Figure 4, we have

$$q(a_3^{K_7}) = 0, \quad q(a_2^{K_6}) = q(a_3^{K_5}). \quad (3.7)$$

At point A , there is no construction for \mathbf{v}_2 . We will construct part of \mathbf{v}_2 for the two vertex-values of q at a boundary point B in Figure 4.

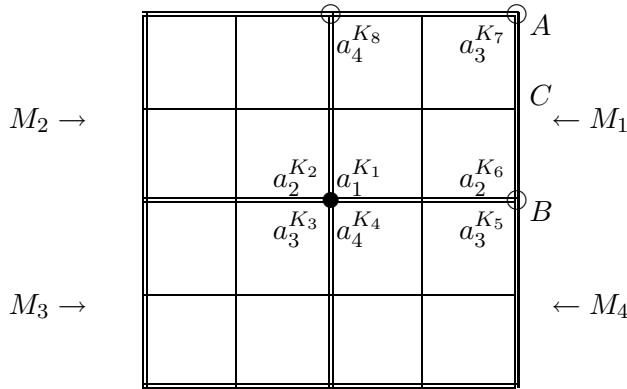


Figure 4: Four macro-elements meeting at a singular vertex, $a_i^{K_i}$, cf. (3.7).

Let the point B in Figure 4 be (x_{i+1}, y_j) . Let

$$\mathbf{v}_{b0} = \begin{cases} \left(q(a_2^{K_6}) \frac{(x_i-x)(x_{i+1}-x)}{(x_{i+1}-x_i)} \frac{(y_{j+1}-y)}{(y_{j+1}-y_j)} \quad 0 \right)^T, & (x, y) \in K_6 \\ \left(q(a_3^{K_5}) \frac{(x_i-x)(x_{i+1}-x)}{(x_{i+1}-x_i)} \frac{(y-y_{j-1})}{(y_j-y_{j-1})} \quad 0 \right)^T, & (x, y) \in K_5 \\ \left(0 \quad 0 \right)^T, & \text{all other } K \in \mathcal{T}_h. \end{cases} \quad (3.8)$$

By the condition (3.7), $\mathbf{v}_{b0} \in \mathbf{V}_h$. By (3.8), we have

$$\nabla \cdot \mathbf{v}_{b0}(a) = \begin{cases} q(a) & a = a_2^{K_6}, a_3^{K_5}, \\ 0 & \text{all other vertices of } M \in \mathcal{M}_h. \end{cases}$$

We note that $\nabla \cdot \mathbf{v}_{b0}(a) \neq 0$ at mid-edge points of M , such as C shown in Figure 4. Further, we preserve the divergence each macro-element, such as

$$\begin{aligned} \int_{M_1} \nabla \cdot \mathbf{v}_{b0} d\mathbf{x} &= \int_{K_6} \nabla \cdot \mathbf{v}_{b0} d\mathbf{x} = \int_{\partial K_6} \mathbf{v}_{b0} \cdot \mathbf{n} ds \\ &= \int_{x_i}^{x_{i+1}} \left(q(a_2^{K_6}) \frac{(x-x_i)(x_{i+1}-x)}{(x_{i+1}-x_i)} \quad 0 \right) \begin{pmatrix} 0 & -1 \end{pmatrix}^T dx = 0. \end{aligned}$$

We compute the semi- H^1 norm of \mathbf{v}_{b0} in two steps.

$$\begin{aligned} \int_{K_6} \left(\frac{\partial \mathbf{v}_{b0}}{\partial x} \right)^2 dx dy &= \frac{1}{9} q^2(a_2^{K_6}) (x_{i+1} - x_i)(y_{j+1} - y_j), \\ \int_{K_6} \left(\frac{\partial \mathbf{v}_{b0}}{\partial y} \right)^2 dx dy &= \frac{1}{30} q^2(a_2^{K_6}) \frac{(x_{i+1} - x_i)^3}{y_{j+1} - y_j}. \end{aligned}$$

On the other side, the L^2 norm and L^∞ norm are equivalent on the reference square $\hat{K} = [-1, 1]^2$ for Q_1 polynomials. There is a constant C such that

$$\int_{\hat{K}} q_1^2 dx dy \geq C q_1^2(1, -1), \quad \forall q_1 \in Q_1.$$

After being scaled by the reference mapping,

$$|\mathbf{v}_{b0}|_{H^1(K_6)}^2 \leq C \left(1 + \frac{(x_{i+1} - x_i)^2}{(y_{j+1} - y_j)^2} \right) q^2(a_2^{K_1}) (x_{i+1} - x_i)(y_{j+1} - y_j) \leq C \|q\|_{L^2(K_6)}^2.$$

Summing over the two elements K_6 and K_5 in Figure 4, it follows that

$$\|\mathbf{v}_{b0}\|_{H^1(\Omega)}^2 \leq C \|q\|_{L^2(\Omega)}, \quad (3.9)$$

where the constant C depends on the maximum aspect ratio of the grid (independent of h). The construction on the other boundary vertex $a_4^{K_8}$ is similar, cf. Figure 4. Next, at an internal vertex, $a_1^{K_1}$ in Figure 4, we need do the above construction three times:

$$\begin{aligned} \mathbf{v}_{b1} &= q(a_3^{K_3}) \mathbf{w}_{K_2, K_3} && \text{(supported on } K_3 \text{ and } K_2), \\ \mathbf{v}_{b2} &= \left(q(a_2^{K_2}) - q(a_3^{K_3}) \right) \mathbf{w}_{K_1, K_2} && \text{(supported on } K_2 \text{ and } K_1), \\ \mathbf{v}_{b3} &= \left(q(a_1^{K_1}) - q(a_2^{K_2}) + q(a_3^{K_3}) \right) \mathbf{w}_{K_1, K_4} && \text{(supported on } K_1 \text{ and } K_4) \\ &= q(a_4^{K_4}) \mathbf{w}_{K_1, K_4} && \text{(by (3.6))}, \end{aligned}$$

where \mathbf{w}_{K_i, K_j} are special functions similar to that in (3.8). Here the second components of \mathbf{w}_{K_2, K_3} and \mathbf{w}_{K_1, K_4} are zero while the first one of \mathbf{w}_{K_1, K_2} is zero. Hence $\int_M \nabla \cdot \mathbf{v}_{bi} = 0$ on each of four macro-elements. We sum all such \mathbf{v}_{bi} to define \mathbf{v}_2 satisfying the requirements of the lemma. Since the support of \mathbf{v}_{bi} are non-overlapping, except that at most 2 nonzero \mathbf{v}_{bi} may occur at each internal vertex,

$$\|\mathbf{v}_2\|_{H^1(\Omega)}^2 \leq 2C \|q\|_{L^2(\Omega)},$$

where C is defined in (3.9). ■

After we match the integrals and the four-vertex values of $q \in P_h$ on macro-elements, we will next match q at mid-edge points on each macro-element.

Lemma 3.3 For any $q \in P_h$ defined in (2.4) such that $\int_M q = 0$ and $q(a_i^M) = 0$ for all $M \in \mathcal{M}_h$, there is a function $\mathbf{v}_3 \in \mathbf{V}_h$ such that

$$\nabla \cdot \mathbf{v}_3(b_i^M) = q(b_i^M) \quad \forall M \in \mathcal{M}_h, \quad (3.10)$$

$$\int_M \nabla \cdot \mathbf{v}_3 = 0 \quad \text{and} \quad \nabla \cdot \mathbf{v}_3(a_i^M) = 0 \quad \forall M \in \mathcal{M}_h, \quad (3.11)$$

$$\|\mathbf{v}_3\|_{H^1(\Omega)^2} \leq C \|q\|_{L^2(\Omega)}. \quad (3.12)$$

Here b_i^M , $1 \leq i \leq 8$, are the eight mid-edge points of macro-element M , and $\{a_i^M\}$ are the four vertices of M .

Proof. There are two types of mid-edge points of macro-elements, such as $b_3^{K_3}$ (on the boundary) and $b_1^{K_6}$ (in the internal), shown in Figure 5. We consider an internal mid-edge point first. By (3.6), see Figure 5,

$$q(b_4^{K_5}) = q(b_1^{K_6}) - q(b_2^{K_1}) + q(b_3^{K_4}). \quad (3.13)$$

We will construct a \mathbf{v}_{m0} to correct q at $b_4^{K_5}$ but not to alter the match made in last lemma at vertices of M , such as A and C shown in Figure 5. Similar to, but different from, (3.8), let

$$\mathbf{v}_{m0} = \begin{cases} \left(\left((q(b_1^{K_6}) - q(b_2^{K_1})) \frac{(x_{i+1}-x)^2}{2(x_{i+1}-x_i)} \frac{(y_{j+1}-y)}{(y_{j+1}-y_j)} \right) 0 \right)^T, & (x, y) \in K_6 \\ \left(\left((q(b_1^{K_6}) - q(b_2^{K_1})) \frac{(x_{i-1}-x)^2}{2(x_i-x_{i-1})} \frac{(y_{j+1}-y)}{(y_{j+1}-y_j)} \right) 0 \right)^T, & (x, y) \in K_1 \\ \left(\left((q(b_1^{K_6}) - q(b_2^{K_1})) \frac{(x_{i-1}-x)^2}{2(x_i-x_{i-1})} \frac{(y-y_{j-1})}{(y_j-y_{j-1})} \right) 0 \right)^T, & (x, y) \in K_3 \\ \left(\left((q(b_1^{K_6}) - q(b_2^{K_1})) \frac{(x_{i-1}-x)^2}{2(x_i-x_{i-1})} \frac{(y-y_{j-1})}{(y_j-y_{j-1})} \right) 0 \right)^T, & (x, y) \in K_5 \\ \left(0 \ 0 \right)^T, & \text{all other } K \in \mathcal{T}_h. \end{cases} \quad (3.14)$$

Here $b_1^{K_6} = (x_i, y_j)$ is assumed.

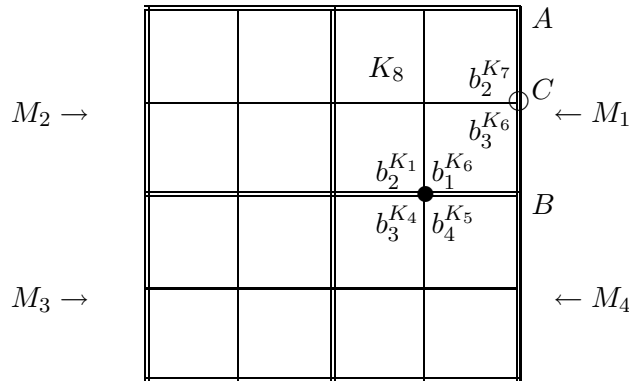


Figure 5: Mid-edge singular points on a macro-element M_1 , cf. (3.7).

By the condition (3.14), $\mathbf{v}_{m0} \in \mathbf{V}_h$. It preserves the divergence each macro-element, such as

$$\int_{M_1} \nabla \cdot \mathbf{v}_{m0} d\mathbf{x} = \int_{\partial M_1} \mathbf{v}_{m0} \cdot \mathbf{n} ds = \int_{x_{i-1}}^{x_{i+1}} \mathbf{v}_{m0}|_{y=y_j} \cdot \begin{pmatrix} 0 \\ -1 \end{pmatrix} dx = 0.$$

Further \mathbf{v}_{m0} reduces the degrees of freedom of q at a singular vertex $b_2^{K_1}$ from 3 to 2. That is, letting $\tilde{q} = q - \nabla \cdot \mathbf{v}_{m0}$, by (3.13) and (3.14),

$$\tilde{q}(b_2^{K_1}) = \tilde{q}(b_1^{K_6}) = q(b_2^{K_1}), \quad \tilde{q}(b_2^{K_1}) = \tilde{q}(b_1^{K_6}) = q(b_2^{K_1}).$$

But it remains that

$$\tilde{q}(a_i^M) = 0 \quad \text{at all corner vertices } a_i^M. \quad (3.15)$$

We note that the construction of \mathbf{v}_{m0} is on four rectangles, but \mathbf{v}_{b0} can be done on two rectangles. Here we have to use fully the property that the first component of v_h is a degree 2 polynomial in x , to preserve (3.15). A calculation like (3.9) shows that

$$\|\mathbf{v}_{m0}\|_{H^1(\Omega)^2} \leq C\|q\|_{L^2(\Omega)}. \quad (3.16)$$

Now, for \tilde{q} , because of (3.15), the situation at the boundary point C is the same as the situation at an internal mid-edge point $b_2^{K_1}$, see Figure 5, i.e., the two values of \tilde{q} at two sides of a mid-edge point are the same. For easier notations, we consider q at a mid-edge boundary point, the boundary node C . By (3.6), $q(b_2^{K_7}) = q(b_3^{K_6})$. Different from (3.8), we have to construct a \mathbf{v}_{m1} on four rectangles, instead of two, in order not to perturb the matches already made by \mathbf{v}_{m0} at mid-edge vertices of M_1 , see Figure 5. This is similar to (3.14):

$$\mathbf{v}_{m1} = \begin{cases} \left(q(b_2^{K_7})(x - x_{i+1}) \frac{(y_{j+1}-y)}{(y_{j+1}-y_j)} & 0 \right)^T, & (x, y) \in K_7 \\ \left(-q(b_2^{K_7}) \frac{(x_{i-1}-x)^2}{(x_i-x_{i-1})^2} \frac{(y_{j+1}-y)}{(y_{j+1}-y_j)} & 0 \right)^T, & (x, y) \in K_8 \\ \left(q(b_2^{K_7})(x - x_{i+1}) \frac{(y-y_{j-1})}{(y_j-y_{j-1})} & 0 \right)^T, & (x, y) \in K_1 \\ \left(-q(b_2^{K_7}) \frac{(x_{i-1}-x)^2}{(x_i-x_{i-1})^2} \frac{(y-y_{j-1})}{(y_j-y_{j-1})} & 0 \right)^T, & (x, y) \in K_6 \\ \left(0 & 0 \right)^T, & \text{all other } K \in \mathcal{T}_h. \end{cases}$$

Here $b_2^{K_7} = (x_{i+1}, y_j)$ is assumed. As the last two times, it is straightforward to verify that $\mathbf{v}_{m1} \in \mathbf{V}_h$, $\int_{M_1} \nabla \cdot \mathbf{v}_{m1} = 0$ and

$$\|\mathbf{v}_{m1}\|_{H^1} \leq C\|q\|_{L^2}. \quad (3.17)$$

By the construction, we have

$$\nabla \cdot \mathbf{v}_{m1}(a) = \begin{cases} q(a) & a = b_2^{K_7}, b_3^{K_6}, \\ 0 & \text{rest corner vertices and mid-edge points of } M \in \mathcal{M}_h. \end{cases}$$

Finally, we add all such \mathbf{v}_{m0} (one for each internal mid-edge point of M) and \mathbf{v}_{m1} (one for each of four mid-edge points of M) to get

$$\mathbf{v}_3 = \sum \mathbf{v}_{m0} + \sum \mathbf{v}_{m1}.$$

Since the nonzero overlapping is 4 in \mathbf{v}_3 (four times by each component of \mathbf{v}_3), we have

$$\|\mathbf{v}_3\|_{H^1(\Omega)^2} \leq 2\sqrt{2}\|q\|_{L^2(\Omega)}.$$

where C is from (3.16) and (3.17). The proof is completed. \blacksquare

The last step is to match q at the center point on each macro-element. After doing so, we would get the following inf-sup condition.

Theorem 3.1 Let $k \geq 2$. The mixed finite element pair (\mathbf{V}_h, P_h) defined in (2.3) and (2.4) is stable, i.e., the inf-sup condition (3.1) holds.

Proof. For any $q \in P_h$, we construct a $\mathbf{v} \in \mathbf{V}_h$ to satisfy (3.1). By (3.2), there is a $\mathbf{v}_1 \in \mathbf{V}_h$ such that

$$\int_M (q - \nabla \cdot \mathbf{v}_1) = 0 \quad \forall M \in \mathcal{M}_h,$$

$$\|\mathbf{v}_1\|_{H^1(\Omega)^2} \leq C_1 \|q\|_{L^2(\Omega)}.$$

By (3.3), there is a stable $\mathbf{v}_2 \in \mathbf{V}_h$ such that

$$[\nabla \cdot \mathbf{v}_2 - (q - \nabla \cdot \mathbf{v}_1)]|_M (a_i^M) = 0 \quad \forall M \in \mathcal{M}_h \text{ and for 4 vertices } a_i^M \text{ of } M,$$

$$\|\mathbf{v}_2\|_{H^1(\Omega)^2} \leq C_2 \|q - \nabla \cdot \mathbf{v}_1\|_{L^2(\Omega)}.$$

By (3.10), there is a $\mathbf{v}_3 \in \mathbf{V}_h$ such that

$$(\nabla \cdot \mathbf{v}_3 - (q - \nabla \cdot \mathbf{v}_1 - \nabla \cdot \mathbf{v}_2)) (b_j^M) = 0 \quad \text{for all 12 corner}$$

$$\text{and mid-edge points } b_j^M \text{ of } M,$$

$$\|\mathbf{v}_3\|_{H^1(\Omega)^2} \leq C_3 \|q - \nabla \cdot \mathbf{v}_1 - \nabla \cdot \mathbf{v}_2\|_{L^2(\Omega)}.$$

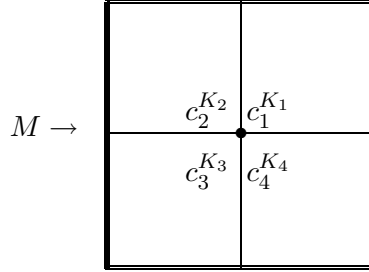


Figure 6: The center singular point of a macro-element M , cf. (3.7).

For $\hat{q} = q - \nabla \cdot (\mathbf{v}_1 + \mathbf{v}_2 + \mathbf{v}_3)$, we have, on each macro-element M , $\hat{q}(a) = 0$ at all 12 points except the center point $c_i^{K_j}$, shown in Figure 6. For simplicity, let us assume the four rectangles K_i of M are squares. Then, by (3.7) and $\int_M \hat{q} = 0$, the degrees of freedom of \hat{q} at the center point of M would be 2, i.e., cf. Figure 6,

$$\hat{q}(c_2^{K_2}) = -\hat{q}(c_4^{K_4}), \quad \hat{q}(c_1^{K_1}) = -\hat{q}(c_3^{K_3}).$$

We construct a \mathbf{v}_4 whose divergence is zero on ∂M and matches the two values of \hat{q} at the center point. Let, cf. Figure 6,

$$\mathbf{v}_{c1} = \begin{cases} \left(\frac{\hat{q}(c_4^{K_4}) - \hat{q}(c_3^{K_3})}{2} \frac{(x_{i+1}-x)^2}{2(x_{i+1}-x_i)} \frac{(y_{j+1}-y)}{(y_{j+1}-y_j)} \quad 0 \right)^T, & \text{on } K_1, \\ \left(\frac{\hat{q}(c_4^{K_4}) - \hat{q}(c_3^{K_3})}{2} \frac{(x_{i+1}-x)^2}{2(x_{i+1}-x_i)} \frac{(y-y_{j-1})}{(y_j-y_{j-1})} \quad 0 \right)^T, & \text{on } K_4, \\ \left(\frac{\hat{q}(c_4^{K_4}) - \hat{q}(c_3^{K_3})}{2} \frac{(x-x_i)^2}{2(x_i-x_{i-1})} \frac{(y-y_{j-1})}{(y_j-y_{j-1})} \quad 0 \right)^T, & \text{on } K_3, \\ \left(\frac{\hat{q}(c_4^{K_4}) - \hat{q}(c_3^{K_3})}{2} \frac{(x-x_i)^2}{2(x_i-x_{i-1})} \frac{(y_{j+1}-y)}{(y_{j+1}-y_j)} \quad 0 \right)^T, & \text{on } K_2, \\ \mathbf{0}, & \text{elsewhere,} \end{cases}$$

$$\mathbf{v}_{c2} = \begin{cases} \left(0 \quad \frac{\hat{q}(c_3^{K_3}) + \hat{q}(c_4^{K_4})}{2} \frac{(x_{i+1}-x)}{(x_{i+1}-x_i)} \frac{(y_{j+1}-y)^2}{2(y_{j+1}-y_j)} \right)^T, & \text{on } K_1, \\ \left(0 \quad \frac{\hat{q}(c_3^{K_3}) + \hat{q}(c_4^{K_4})}{2} \frac{(x-x_{i-1})}{(x_i-x_{i-1})} \frac{(y_{j+1}-y)^2}{2(y_{j+1}-y_j)} \right)^T, & \text{on } K_2, \\ \left(0 \quad \frac{\hat{q}(c_3^{K_3}) + \hat{q}(c_4^{K_4})}{2} \frac{(x-x_{i-1})}{(x_i-x_{i-1})} \frac{(y-y_{j-1})^2}{2(y_j-y_{j-1})} \right)^T, & \text{on } K_3, \\ \left(0 \quad \frac{\hat{q}(c_3^{K_3}) + \hat{q}(c_4^{K_4})}{2} \frac{(x_{i+1}-x)}{(x_{i+1}-x_i)} \frac{(y-y_{j-1})^2}{2(y_j-y_{j-1})} \right)^T, & \text{on } K_4, \\ \mathbf{0}, & \text{elsewhere,} \end{cases}$$

where we assume $c_3^{K_3} = (x_i, y_j)$. Then we let $\mathbf{v}_4 = \sum(\mathbf{v}_{c1} + \mathbf{v}_{c2})$. By the construction, we have

$$\hat{q} - \nabla \cdot \mathbf{v}_4 \equiv 0, \quad \|\mathbf{v}_4\|_{H^1} \leq C_4 \|\hat{q}\|_{L^2}.$$

Finally, we define

$$\mathbf{v} = -\mathbf{v}_1 - \mathbf{v}_2 - \mathbf{v}_3 - \mathbf{v}_4.$$

It follows that

$$\begin{aligned} \|\mathbf{v}\|_{H^1(\Omega)^2} &\leq \|\mathbf{v}_1\|_{H^1(\Omega)^2} + \|\mathbf{v}_2\|_{H^1(\Omega)^2} + \|\mathbf{v}_3\|_{H^1(\Omega)^2} + \|\mathbf{v}_4\|_{H^1(\Omega)^2} \\ &\leq C_1 \|q\|_{L^2(\Omega)} + C_2 (\|q\|_{L^2(\Omega)} + \|\mathbf{v}_1\|_{H^1(\Omega)^2}) \\ &\quad + C_3 (\|q\|_{L^2(\Omega)} + \|\mathbf{v}_1\|_{H^1(\Omega)^2} + \|\mathbf{v}_2\|_{H^1(\Omega)^2}) \\ &\quad + C_4 (\|q\|_{L^2(\Omega)} + \|\mathbf{v}_1\|_{H^1(\Omega)^2} + \|\mathbf{v}_2\|_{H^1(\Omega)^2} + \|\mathbf{v}_3\|_{H^1(\Omega)^2}) \\ &\leq (C_1 + C_2 + C_3 + C_4 + C_1 C_2 + \dots) \|q\|_{L^2(\Omega)} \end{aligned}$$

and that

$$\begin{aligned} b(\mathbf{v}, q) &= (-\nabla \cdot \mathbf{v}, q) = \|q\|_{L^2(\Omega)}^2 \\ &\geq (C_1 + C_2 + C_3 + C_4 + C_1 C_2 + \dots)^{-1} \|\mathbf{v}\|_{H^1(\Omega)^2} \|q\|_{L^2(\Omega)}. \end{aligned}$$

(3.1) is proved with $C \geq (C_1 + C_2 + \dots)^{-1}$. ■

Corollary 3.1 *The discrete pressure space (2.4) is characterized by*

$$P_h = \left\{ q \mid q|_K \in Q_1 \ \forall K \in \mathcal{T}_h; \int_{\Omega} q = 0; \sum_{i=1}^{i_0} (-1)^i q(a_i^{K_i}) = 0 \right\}, \quad (3.18)$$

where $a_i^{K_i}$ are defined in (3.6), and $i_0 = 4$ at an internal vertex, but i_0 may be 1 or 2 at the boundary.

Proof. In the proof of Theorem 3.1, we constructed a $\mathbf{v} = -\mathbf{v}_1 - \mathbf{v}_2 - \mathbf{v}_3 - \mathbf{v}_4$ for any q_h in the set of (3.18), such that $\nabla \cdot \mathbf{v} = -q_h$. Thus the P_h defined in (3.18) is a subset of that P_h defined in (2.4). On the other side, by the proof of Lemma 3.2, we known that $\nabla \cdot \mathbf{v}_h$ satisfies the constraints in (3.18) for all $\mathbf{v}_h \in \mathbf{V}_h$. ■

Theorem 3.2 *The discrete solution (\mathbf{u}_h, p_h) of (2.5) approximate that of (2.2) in the optimal order:*

$$\|\mathbf{u} - \mathbf{u}_h\|_{H^1(\Omega)^2} + \|p - p_h\|_{L^2(\Omega)} \leq Ch^{\min\{1, r\}} (\|\mathbf{u}\|_{H^{r+1}(\Omega)^2} + \|p\|_{H^r(\Omega)}), \quad r > 0. \quad (3.19)$$

Proof. By the inf-sup condition (3.1) and the standard mixed finite element theory [21], it follows that

$$\begin{aligned} \|\mathbf{u} - \mathbf{u}_h\|_{H^1(\Omega)^2} + \|p - p_h\|_{L^2(\Omega)} &\leq C \left(\inf_{\mathbf{v}_h \in \mathbf{V}_h} \|\mathbf{u} - \mathbf{v}_h\|_{H^1(\Omega)^2} + \inf_{q_h \in P_h} \|p - q_h\|_{L^2(\Omega)} \right) \\ &\leq C \left(\inf_{\mathbf{v}_h \in \tilde{\mathbf{V}}_h} \|\mathbf{u} - \mathbf{v}_h\|_{H^1(\Omega)^2} + \inf_{q_h \in \tilde{P}_h} \|p - q_h\|_{L^2(\Omega)} \right) \end{aligned}$$

where \tilde{P}_h is the space of continuous Q_1 polynomials with mean value zero:

$$\tilde{P}_h = \left\{ q_h \in C^0(\Omega) \mid \int_{\Omega} q_h = 0, q_h|_K \in Q_1 \ \forall K \in \mathcal{T}_h \right\}. \quad (3.20)$$

We note that $\tilde{P}_h \subset P_h$, because functions in \tilde{P}_h satisfy the constraints in (3.18). The theorem is proven as both spaces \mathbf{V}_h and \tilde{P}_h provide the optimal order of approximation. \blacksquare

4 Numerical tests

In this section, we report some results of numerical experiments on the $Q_{2,1;1,2}$ element for the stationary Stokes equations (2.1) on the unit square $\Omega = [0, 1]^2$. The grids \mathcal{T}_h are depicted in Figure 2, i.e., each squares are refined into 4 sub-squares each level. The initial grid, level one grid, is simply one unit square. The computed inf-sup constants, i.e., the maximum constant C in (3.1), are listed in Table 1. This confirms Theorem 3.1 that the $Q_{2,1;1,2}$ element is stable.

Table 1: The inf-sup constants for (3.1) on Figure 2 grids.

level	$\dim V_h$	$\dim P_h$	C in (3.1)
2	6	6	0.60615
3	42	38	0.54410
4	210	174	0.52552
5	930	734	0.52069
6	3906	3006	0.51931

We choose a simple exact solution for the Stokes equations (2.1):

$$\mathbf{u} = \nabla \times g, \quad p = -g_{xx}. \quad (4.1)$$

Here

$$g = 2^8(x - x^2)^2(y - y^2)^2.$$

So we can compute the right hand side function \mathbf{f} for (2.1) as

$$\mathbf{f} = -\Delta \nabla \times g - \nabla g_{xx} = \begin{pmatrix} -g_{yxx} - g_{yyy} - g_{xxx} \\ g_{xxx} + g_{xyy} - g_{yxx} \end{pmatrix}, \quad (4.2)$$

In Table 2 we list various norms and orders of convergence for the finite element solutions in the spaces $\mathbf{V}_h \times P_h$ defined in (2.3)-(2.4). Here we do enough iterated penalty iterations (cf. [25, 30]) until the iterative error is smaller than the truncation error each time. We plot

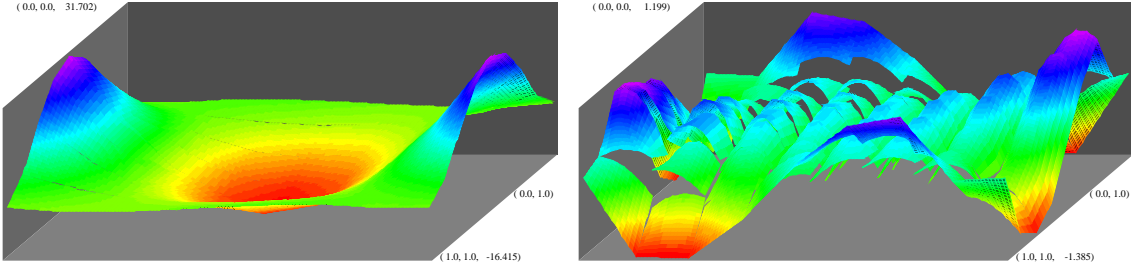


Figure 7: The solution p_h and the error on the level 4 grid.

Table 2: The errors $\mathbf{e}_h = \mathbf{u} - \mathbf{u}_I$ and $\epsilon_h = p - p_I$ for the $Q_{2,1;1,2}$ div-free element.

	$ \mathbf{e}_h _{H^1}$	h^n	$ \mathbf{e}_h _{L^2}$	h^n	$ \mathbf{e}_h _{l_\infty}$	h^n	$\ \epsilon_h\ _{L^2}$	h^n	$\ \epsilon_h\ _{l_\infty}$	h^n
2	0.00000		0.000000		0.000000		2.9212		7.20000	
3	1.21102		0.107128		0.199477		1.8436	0.7	6.66677	0.1
4	0.31197	2.0	0.027245	2.0	0.045769	2.1	0.4541	2.0	1.44615	2.2
5	0.07836	2.0	0.006825	2.0	0.011004	2.1	0.1129	2.0	0.37275	2.0
6	0.01961	2.0	0.001707	2.0	0.002709	2.0	0.0282	2.0	0.09273	2.0
7	0.00490	2.0	0.000427	2.0	0.000676	2.0	0.0070	2.0	0.02346	2.0
8	0.00123	2.0	0.000107	2.0	0.000169	2.0	0.0018	2.0	0.00590	2.0
9	0.00031	2.0	0.000027	2.0	0.000043	2.0	0.0004	2.0	0.00148	2.0

the solution p_h and the error on the level 4 grid in Figure 7. In Table 2, the velocity errors are denoted by $\mathbf{e}_h = \mathbf{u} - \mathbf{u}_I$ where \mathbf{u} is defined in (4.1) and \mathbf{u}_I is an interpolation of \mathbf{u} . The pressure errors in Table 2 are listed as $\epsilon_h = p - p_I$ for p defined in (4.1) and p_I an interpolation. The standard optimal order of convergence, provided in Theorem 3.2, for $\|\mathbf{e}_h\|_{H^1}$ and $\|\epsilon_h\|_{L^2}$ is 1. But we obtain an order two convergence for them, due to the superconvergence on uniform grids.

Table 3: The errors $\mathbf{e}_h = \mathbf{u} - \mathbf{u}_I$ and $\epsilon_h = p - p_I$ for the Q_1/P_0 element.

	$ \mathbf{e}_h _{H^1}$	h^n	$ \mathbf{e}_h _{L^2}$	h^n	$ \mathbf{e}_h _{l_\infty}$	h^n	$\ \epsilon_h\ _{L^2}$	h^n	$\ \epsilon_h\ _{l_\infty}$	h^n
3	0.95466		0.103190		0.226339		3.9982		5.02027	
4	0.33184	1.5	0.037889	1.4	0.051456	2.1	1.0103	2.0	1.91412	1.4
5	0.08849	1.9	0.010256	1.9	0.013588	1.9	0.1723	2.6	0.44291	2.1
6	0.02247	2.0	0.002613	2.0	0.003376	2.0	0.0308	2.5	0.15302	1.5

Finally, we make a brief comparison between the new divergence-free element and the most popular Q_1/P_0 element, cf. the references in [19]. The convergence data for the Q_1/P_0 element are listed in Table 3. We have a super-convergence for the Q_1/P_0 element. The degree of freedom for the velocity in $Q_{2,1;1,2}$ is about twice of that in Q_1/P_0 . But as we do not introduce the pressure space P_h in computation, the total unknowns in the linear system for the $Q_{2,1;1,2}$ divergence-free element are about the same as that for the Q_1/P_0 element. The convergence of $Q_{2,1;1,2}$ is better than that of the Q_1/P_0 element, seen on level 6 computation in

Tables 2 and 3. On the other side, the linear system for the divergence-free $Q_{2,1;1,2}$ element is much easier to be solved, as we solve positive-definite systems each step, thanks to the iterated penalty method.

References

- [1] M. Ainsworth and P. Coggins, *A uniformly stable family of mixed hp-finite elements with continuous pressures for incompressible flow*, IMA J. Num. Anal. 22 (2002), 307–327 .
- [2] D. N. Arnold and J. Qin, *Quadratic velocity/linear pressure Stokes elements*, in Advances in Computer Methods for Partial Differential Equations VII, ed. R. Vichnevetsky and R.S. Steplemen, 1992.
- [3] D. Arnold, L.R. Scott and M. Vogelius, *Regular inversion of the divergence operator with Dirichlet conditions on a polygon*, Ann. Sc. Norm. Super Pisa, C1. Sci., IV Ser., 15(1988), 169–192
- [4] C. Bernardi and Y. Maday, *Uniform inf-sup conditions for the spectral discretization of the Stokes problem*, Math. Meth. Appl. Sci. 9 (1999), 395–414.
- [5] C. Bernardi and B. Raugel, *Analysis of some finite elements of the Stokes problem*, Math. Comp., 44 (1985), 71–79.
- [6] S.C. Brenner, *An optimal-order multigrid method for P1 nonconforming finite elements*, Math. Comp. 52 (1989), 1–15.
- [7] S.C. Brenner and L.R. Scott, *The Mathematical Theory of Finite Element Methods*, Springer-Verlag, New York, 1994.
- [8] F. Brezzi and M. Fortin, *Mixed and hybrid finite element methods*, Springer, 1991.
- [9] F. Brezzi and R. Falk, *Stability of higher-order Hood-Taylor Methods*, SIAM J. Numer. Anal. 28 (1991), no. 3, 581–590.
- [10] J. Carrero, B. Cockburn and D. Schötzau, *Hybridized globally divergence-free LDG methods. I. The Stokes problem*, Math. Comp. 75 (2006), 533–563.
- [11] P.G. Ciarlet, *The Finite Element Method for Elliptic Problems*, North-Holland, Amsterdam, 1978.
- [12] B. Cockburn, F. Li and C.-W. Shu, *Locally divergence-free discontinuous Galerkin methods for the Maxwell equations*, J. Comput. Phys. 194 (2004), 588–610.
- [13] M. Fortin and R. Glowinski, *Augmented Lagrangian Methods: Applications to the Numerical Solution of Boundary-value Problems*, North Holland, Amsterdam, 1983.
- [14] O.Karakashian and T. Katsaounis, *Numerical simulation of incompressible fluid flow using locally solenoidal elements*. Comput. Math. Appl. 51 (2006), 1551–1570.
- [15] F. Li and C.-W. Shu, *Locally divergence-free discontinuous Galerkin methods for MHD equations*, J. Sci. Comput. 22/23 (2005), 413–442.
- [16] J.-C. Nédélec, *Mixed finite elements in R^3* , Numer. Math. 35 (1980), 315–341.

- [17] P. Oswald, *Remarks on multilevel bases for divergence-free finite elements*, Numerical Algorithms 27 (2001), 131-152.
- [18] J. Qin , *On the convergence of some low order mixed finite elements for incompressible fluids*, Thesis, Pennsylvania State University, 1994.
- [19] J. Qin and S. Zhang, *Stability of the finite elements $9/(4c+1)$ and $9/5c$ for stationary Stokes equations*, Computers and Structures, 84 (2005), 70–77.
- [20] J. Qin and S. Zhang, *Stability and approximability of the $P1-P0$ element for Stokes equations*, Int. J. Numer. Meth. Fluids, 54 (2007), 497–515.
- [21] P. A. Raviart and V. Girault, *Finite element methods for Navier-Stokes equations*, Springer, 1986.
- [22] P. Raviart and J. Thomas, *A mixed finite element method for 2nd order elliptic problems*, in Mathematics Aspects of Finite Element Methods, Lecture Notes in Math. 606, SpringerVerlag, New York, 1977, 292-315.
- [23] L. R. Scott and M. Vogelius, *Norm estimates for a maximal right inverse of the divergence operator in spaces of piecewise polynomials*, RAIRO, Modelisation Math. Anal. Numer. 19 (1985), 111–143.
- [24] L. R. Scott and M. Vogelius, *Conforming finite element methods for incompressible and nearly incompressible continua*, in Lectures in Applied Mathematics 22, 1985, 221–244.
- [25] L. R. Scott and S. Zhang, *Finite element interpolation of nonsmooth functions satisfying boundary conditions* , Math. Comp. 54 (1990), 483–493.
- [26] L. R. Scott and S. Zhang, *Multilevel Iterated Penalty Method for Mixed Elements*, the Proceedings for the Ninth International Conference on Domain Decomposition Methods, 133-139, Bergen, 1998.
- [27] R. Stenberg and M. Suri, *Mixed hp finite element methods for problems in elasticity and Stokes flow*, Numer. Math. 72 (1996), 367–389.
- [28] X. Ye and G. Anderson, *The derivation of minimal support basis functions for the discrete divergence operator*, J. Compu. Appl. Math. 61 (1995), 105–116.
- [29] S. Zhang, *A new family of stable mixed finite elements for 3D Stokes equations*, Math. Comp. 74 (2005), 250, 543–554.
- [30] S. Zhang, *On the $P1$ Powell-Sabin divergence-free finite element for the Stokes equations*, J. Comp. Math., 26 (2008), 456-470.
- [31] S. Zhang, *A family of $Q_{k+1,k} \times Q_{k,k+1}$ divergence-free finite elements on rectangular grids*, SIAM J. Num. Anal., 47 (2009), 2090-2107.

Hunan Key Laboratory for Computation and Simulation in Science and Engineering, Xiangtan University, China, 411105. huangyq@xtu.edu.cn.
 Department of Mathematical Sciences, University of Delaware, DE 19716. szhang@udel.edu.